Journal of Clinical Virology xxx (2009) xxx–xxx

Contents lists available at ScienceDirect

Journal of Clinical Virology

journal homepage: www.elsevier.com/locate/jcv

Cold oxygen plasma technology efficiency against different airborne respiratory viruses

O. Terrier[a,b,c], B. Essere[a,b,c], M. Yver[a,b,c], M. Barthélémy[a,b,c], M. Bouscambert-Duchamp[a,b,c,d], P. Kurtz[e], D. VanMechelen[e], F. Morfin[a,b,c,d], G. Billaud[a,b,c,d], O. Ferraris[a,b,c], B. Lina[a,b,c,d], M. Rosa-Calatrava[a,b,c], V. Moules[a,b,c,*]

[a] Université de Lyon, F-69000 Lyon, France
[b] Université Lyon 1, Faculté de médecine RTH Laennec, France
[c] CNRS FRE 3011 VirPath, Virologie et Pathologie Humaine, F-69008 Lyon, France
[d] Laboratoire de virologie, centre de Biologie et de Pathologie Est, Hospices Civils de Lyon, 59 boulevard Pinel, 69677 Bron cedex, Lyon, France
[e] Biozone Europe, 1 rue notre dame, F-59300 Valenciennes, France

ARTICLE INFO

Article history:
Received 16 December 2008
Received in revised form 24 March 2009
Accepted 25 March 2009

Keywords:
Influenza
Parainfluenza
Respiratory syncytial virus
Airborne transmission
Cold plasma
Germicidal ultraviolet light

ABSTRACT

Background: Respiratory infections caused by viruses are major causes of upper and lower respiratory tract infections. They account for an important mortality and morbidity worldwide. Amongst these viruses, influenza viruses and paramyxoviruses are major pathogens. Their transmission is mainly airborne, by direct transmission through droplets from infected cases.
Objectives: In the context of an influenza pandemic, as well as for the reduction of nosocomial infections, systems that can reduce or control virus transmission will reduce the burden of this disease. It may also be part of the strategy for pandemic mitigation.
Study design: A new system based on physical decontamination of surface and air has been developed. This process generates cold oxygen plasma (COP) by subjecting air to high-energy deep-UV light. To test its efficiency, we have developed an experimental device to assess for the decontamination of nebulized respiratory viruses. High titer suspensions of influenza virus type A, human parainfluenza virus type 3 and RSV have been tested.
Results: Different experimental conditions have been evaluated against these viruses. The use of COP with an internal device allowed the best results against all viruses tested. We recorded a reduction of 6.5, 3.8 and 4 log(10) TCID50/mL of the titre of the hPIV-3, RSV and influenza virus A (H5N2) suspensions.
Conclusions: The COP technology is an efficient and innovative strategy to control airborne virus dissemination. It could successfully control nosocomial diffusion of respiratory viruses in hospital setting, and could be useful for the reduction of influenza transmission in the various consultation settings implemented for the management of cases during a pandemic.

1. Background

Respiratory syncytial virus (RSV) and human parainfluenza virus type 3 (hPIV-3) infections are two leading causes of lower respiratory illness (LRI) in young children and also in elderly.[1,2] These infections are associated to high morbidity. Global annual mortality worldwide for RSV, for example, is estimated to be 160,000 and many efforts are actually done in order to develop vaccines and antiviral drugs against these viruses.[3,4] Influenza virus is one of the most important viruses responsible for upper respiratory tract infection regarding morbidity and mortality. Prevention and treatment of influenza viruses rely on inactivated vaccines and antiviral drugs. The prospect of future influenza pandemics, potentially caused by avian influenza has raised the question of pandemics preparedness.[5,6]

Airborne transmission, either direct or secondary, has been postulated to be involved in the dissemination and spread of several microorganisms.[7] Several reports have shown that fine particle aerosols may play a role in respiratory virus infection. It is now well established for influenza virus, but it may not be the primary way of spreading for RSV and hPIV-3.[7,8] To protect human population, several air disinfection systems have been developed, based on different technologies. Classic approaches consist in air filtration,[9] ionization,[10] and ultraviolet irradiation.[11] Other recent approaches implicate air oxi-

* Corresponding author at: Université Lyon 1, F-69000 Lyon, France.
Tel.: +33 4 78 77 10 36; fax: +33 4 78 77 87 51.
E-mail address: Vincent.moules@recherche.univ-lyon1.fr (V. Moules).

1386-6532/$ – see front matter © 2009 Elsevier B.V. All rights reserved.
doi:10.1016/j.jcv.2009.03.017

dation by photocatalytic process,[12,13] ozone [14] or plasma-based disinfection.

Gas plasmas can be considered as the fourth state of matter, following by order of increasing energy, the solid, liquid and gaseous states. Man-made cold gas plasmas are usually produced by subjecting a gas to an electric field. Gas plasmas are composed of ions, electrons, uncharged particles such as atoms, molecules (e.g. O_3) and radicals (OH-, NO-, etc.).[15] These ions and uncharged particles can be in an excited state and can become to a normal state by emitting a photon or through collisions with a surface for example. These events can induce chemical reactions such as oxidations and lipid/protein peroxidations.[15] The possibility to use plasma-sterilizing properties was first introduced in the end of 60s and first works with a plasma made with oxygen were proposed in 1989. Nelson and Berger[16] have shown that O_2 plasma could be a very efficient biocidal tool against bacteria. More recently, Biozone scientific firm has developed a new process for the generation of a cold oxygen plasma (COP) by subjecting air by high-energy deep-UV light with a effective radiation spectrum between 180 nm and 270 nm. This cold gas plasma is composed of several species like negative and positive ions, free radical molecules, electron, UV-photons and ozone. The ozone production is controlled and maintained to a maximum level of 0.04 ppmv (parts per million by volume). This technology is dedicated to be used in human environment for the decontamination of both surface and air.

2. Objectives

To our knowledge, no attempts have been made to evaluate the efficiency of cold oxygen plasma against virus and more precisely airborne respiratory viruses. To address this issue we have set up an experimental device in the purpose of testing the efficiency of Biozone technology COP against nebulizated preparation of three respiratory viruses of significant clinical importance: RSV, hPIV-3 and A (H5N2) influenza viruses.

3. Study design

3.1. Cells and viruses

LLC-MK2 cells (Monkey kidney cells) were obtained from American type culture collection (ATCC reference CCL-7) and were grown in Eagle's minimal essential medium (EMEM) with 5% foetal calf serum. MDCK (Madin-Darby canine kidney cells) were obtained from American type culture collection (ATCC reference CCL-34) and were grown in ultra MDCK medium (Lonza-Biowhittaker). RSV-A Long strain and hPIV-3 C-243 strain were obtained from the ATCC (respectively ATCC VR-26 and ATCC VR-93). Since the influenza A (H5N1) virus is strongly pathogenic, the study was performed with the A (H5N2) strain chosen as the conventional research model for the influenza virus A (H5N1) strain (H5N2 A/Finch/England/2051/2001).

3.2. Viral production and purification

In order to produce large quantities of hPIV-3 and RSV, three 175 cm^2 flasks of LLC-MK2 cells were infected for each virus at a multiplicity of Infection (MOI) of 10^{-3} [17] and supernatants were harvested 3 days post-infection. After a centrifugation at 1200 × *g* at 4 °C for 10 min, supernatants were centrifuged at 25,000 × *g* at 4 °C for 2 h on a 20% saccharose cushion in phosphate buffered saline (PBS; pH 7.4). Viral pellets were resuspended in 50 mL of PBS; pH 7.4 and stocked at 4 °C before nebulization step. Influenza A (H5N2) strain was cultivated on MDCK cells and the viral suspension was prepared in a same way as hPIV-3 and RSV.

3.3. Cold oxygen plasma experimental device

The efficiency of the gas plasma process in air disinfection was studied directly by a pilot reaction core manufactured by Biozone scientific. A schematic drawing of the testing system is depicted in Fig. 1. The reaction core is composed of external and internal cold oxygen plasma device (COP) and an internal classic UV-C lamp (254 nm).

The system consists of a one-pass flow tunnel with a reaction core to be tested situated inline such that air samples can be taken before and after the reaction core. For safety, the entire system was installed in a BSL3 laboratory with the entry and exit of the flow system located inside biological safety hoods within the laboratory. Samplers to determine upstream and downstream outlet airborne levels of infectious virus where also located inside safety hoods. At the entry of the flow tunnel, a viral aerosol suspension was generated using a 6-jet Collision spray nebulizer (Model CN311, BGI, INC). The suspension was aerosolized by applying compressed air to the Collision nebulizer at 1.8 bars of pressure. Under these conditions, the mean diameter of the droplets is 1.9 μm. During these tests the air speed through the system was stabi-

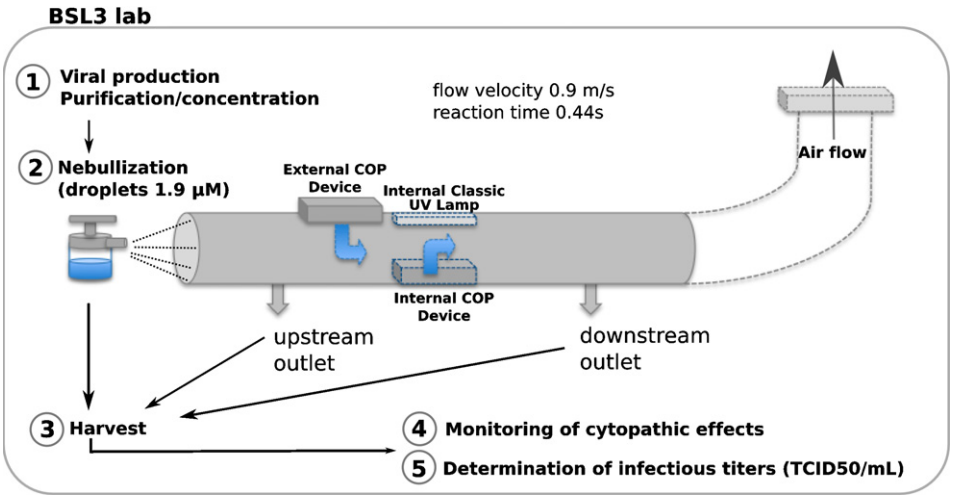

Fig. 1. Schematic representation of the experimental device and strategy used in this study.

Please cite this article in press as: Terrier O, et al. Cold oxygen plasma technology efficiency against different airborne respiratory viruses. *J Clin Virol* (2009), doi:10.1016/j.jcv.2009.03.017

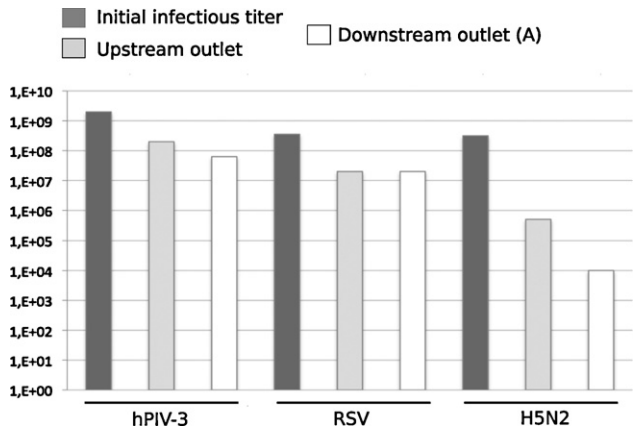

Fig. 2. Evaluation of the viral loss due to the nebulization in the experimental device. The infectious titers (TCID50/mL) of the suspensions harvested at the upstream and the downstream outlets are compared with the initial infectious titer of the viral suspensions, which have been nebulizated, for hPIV-3, RSV and A (H5N2) influenza.

lized and fixed at 0.9 m/s. The virus flow was sampled during 3 min using a sampling pump and then focused onto 3 mL of collection fluid (phosphate buffer saline) in 50 mL sterile plastic tube.

Three different experimental conditions were tested four times (Fig. 3): (B) the internal classic UV germicide UV-C light lamp, (C) a COP from an external device (gas plasma only) and (D) a COP from an internal device (gas plasma and UV light).

3.4. Determination of viral infectious titers

The amount of infectious virus in each batch was performed by limit-dilution titration test and determination of the dilution of virus required to infect 50% of inoculated cells (TCID50/mL).[18] For this purpose, virally induced cytopathic effects (CPE) were checked until 96–120 h post-infection.

4. Results

4.1. Evaluation of viral load reduction due to the nebulization in the experimental system (Fig. 2)

We first evaluated the load reduction of infectious particles during the nebulization in our experimental device. The first experiment was a blind test with no UV-C light or ozone produced into the virus stream. The Collison nebulizer was filled with 30 mL of influenza A (H5N2) or RSV or hPIV-3 purified viral suspensions, with infectious titers of, respectively $10^{8.5}$, $10^{8.55}$ and $10^{9.3}$ TICD50/mL.

After 30 min of stabilisation, four samples were taken alternatively at the upstream outlet and at the downstream outlet, and this operation has been repeated four times to check the reproducibility. The objective was to check that infectious titers, in the suspensions harvested at upstream and downstream outlet (Fig. 1), were high enough to further evaluate the effect of different experimental conditions (e.g. UV-C/COP/COP + UV). First preliminary results have shown that the initial infectious titers had to be very high before nebulization, which implicated concentration/purification steps after viral production.

The loss of infectious particles between the initial infectious titer and the upstream outlet for hPIV-3, RSV and influenza virus A (H5N2) was respectively of the order of 0, 1.25, and 2.8 log(10) TCID50/mL (Fig. 2). The decrease of amount of virus was very important (more than 99.8% for influenza virus A (H5N2)) but the upstream outlet infectious titers still represented non-negligible values ($10^{9.3}$, $10^{7.3}$, and $10^{5.7}$ respectively for hPIV-3, RSV and influenza virus A (H5N2), Fig. 2). We then measured the viral loss between upstream and downstream outlets. Surprisingly, there was no measurable loss for RSV between the two outlets. The loss of infectious particles between the upstream and the downstream outlet for hPIV-3, RSV and influenza virus A (H5N2) was respectively of the order of 0.5, 0, and 1.7 log(10) TCID50/mL (Fig. 2). We also observed marked loss rates at this step, but the downstream outlet infectious titers still represented non-negligible values ($10^{7.8}$, $10^{7.3}$, 10^{4} respectively for hPIV-3, RSV and influenza virus A (H5N2), Fig. 2).

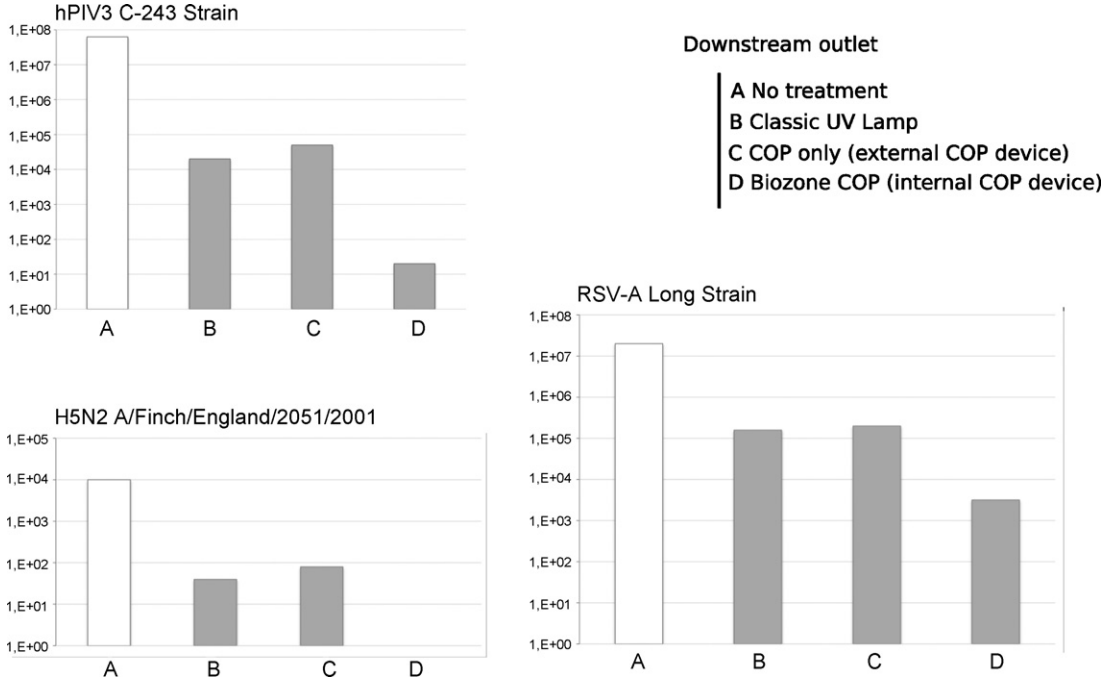

Fig. 3. Determination of downstream outlet infectious titers in different conditions for hPIV-3, RSV and A (H5N2) influenza.

Please cite this article in press as: Terrier O, et al. Cold oxygen plasma technology efficiency against different airborne respiratory viruses. *J Clin Virol* (2009), doi:10.1016/j.jcv.2009.03.017

Table 1
Percentage efficiency of inactivation in the different experimental conditions (B–D, Fig. 3).

	% efficiency		
	Classic UV lamp (B)	COP only (C)	Biozone COP (D)
H5N2	99.60	99.20	>99.99
hPIV-3	99.97	99.92	>99.99
RSV	99.20	99.00	99.98

Altogether, these results have shown that it was possible to harvest, after nebulization of a highly concentrate viral suspension, significant quantities of infectious viruses despite important loss rates.

4.2. Determination of downstream outlet infectious titers in different conditions (Fig. 3)

The downstream outlet infectious titers for each virus, without treatment, previously determined were used as reference values (see Fig. 3A).

We first determined the effect of the classic UV-C light without gas plasma production. The germicidal effects of classic UV-C light lamp allowed a loss of infectious titers, for hPIV-3, RSV and influenza virus A (H5N2) of respectively 3.5, 2.1 and 2.4 log(10) of TCID50/mL (A *versus* B, Fig. 3). We then determined the effect of gas plasma (external COP device) into the virus flow. The ozone concentration was measured to be 0.05 ppmv in this stream complying with all certification levels. When the external COP device was tested, the loss of infectious particles for hPIV-3, RSV and influenza virus A (H5N2) was respectively of the order of 3.1, 2 and 2.1 log(10) TCID50/mL (A *versus* C, Fig. 3). The results between the two experimental conditions A and C were quite comparable. We finally determined the effect of both gas plasma and UV light (external and internal COP devices) into the virus flow. This configuration allowed a more important loss of infectious titers, for hPIV-3, RSV and influenza virus A (H5N2) of respectively 6.5, 3.8 and 4 log(10) TCID50/mL (A *versus* D Fig. 3).

All these results have been expressed as percentage efficiency using the following formula. *Percentage efficiency* = (*infectious titer in A* − *infectious titer in B, C or D*)/(*infectious titer in A*) × 100. The results are shown in Table 1.

4.3. Monitoring of cytopathic effects: an illustration (Fig. 4)

The infectious titers were determined for the observation of infected cell monolayers. In order to illustrate the results presented in Fig. 2, we have monitored the cytopathic effect on MDCK or LLC-MK2 cells, infected with samples harvested at upstream or downstream outlets, when the internal COP device was switched on. From the 3 mL harvested at each outlet, 500 μL was used to infect cell monolayers in 3.5 cm dishes. Representative photographs taken at 72 h post-infection are shown in Fig. 4. Marked cytopathic effects were observed in cell monolayers infected with samples harvested at upstream outlet, for the three viruses. The cell monolayers were totally destructed for influenza virus A (H5N2) (rounded and non-adherent cells, Fig. 4) and only partially for hPIV-3 and RSV, with multiple small characteristic foci (Fig. 4). We have not observed evident cytopathic effect in dishes infected with influenza virus A (H5N2) samples harvested at the downstream outlet; cell monolayers were similar to non-infected ones (MOCK, see Fig. 4). For hPIV-3 and RSV downstream outlet samples, only discrete cytopathic effects were visualised, with small foci (Fig. 4). Our following observations (up to 96 h post-infection) revealed that these foci were probably early syncytial structures (data not shown).

5. Discussion

The aim of this study was to evaluate the efficiency of a cold oxygen plasma generated by the Biozone scientific technology against different respiratory viruses. The main struggle consisted to set up an experimental device, which allowed us to test different treatments of nebulizated viral suspensions. The objective was not to precisely mimic human-produced droplets but the size range appeared to be important. Only limited data are available regarding the size distribution of human-produced droplets. For influenza virus, the average diameter of droplets is of the order of the micrometer,[19,20] which corresponds to the average diameter of droplets generated in our study.

The first set-up experiment (Fig. 2) showed that it was possible to harvest, after nebulization of a high concentrate viral suspension, significant quantities of infectious viruses, despite important loss rates. The important loss rates could be partially explained by a rapid aggregation and consecutive particles settling between the upstream and the downstream outlets and also the liquid impingement samplers have been used to sample the air. The loss rates could be explained by a probable high relative humidity of our experimental condition that is known to affect the infectivity of airborne influenza virus, for example.[21] This feature can be compensated by high initial viral titers.

The UV-C light irradiation capacity to inactivate airborne viruses was not extensively studied in litterature.[11] In early works, Jensen[22] has shown that the inactivation rate of UV-C on influenza (WSN strain) was greater than 99.99%. In our experimental conditions, we have found UV-C inactivation rates for A (H5N2) influenza virus, hPIV-3, and RSV, were respectively of 99.60%, 99.97% and 99.20% (Table 1). These percentages could first appear to be very close but represent lower efficiency considering the infectious titers. These differences could be explained by the number of UV-C lamp used in these two studies; only one in our study *versus* six lamps in the early works by Jensen[22] and also by differences of initial viral titers experimentally used.

In our experiment, gas plasma generated by the Biozone UV lamp is responsible for an important decrease of the viral titer for all the three respiratory viruses. One important element in the composition of a cold gas plasma is the ozone. It is well documented in the scientific literature that ozone–oxygen mixtures inactivate microorganisms including bacteria, fungi and viruses.[23,24] A recent study suggests that ozone inactivation of viruses occurs primarily by peroxidation of both lipid and protein.[24] Enveloped viruses in a thin liquid layer showed extreme sensitivity to ozone using concentrations ranging from 800 ppmv to 1500 ppmv.[24] The Biozone scientific COP only allows the production of 0.04 ppmv of ozone. The effect of such low ozone concentration on nebulizated viral suspensions will be further examined.

Our results showed a slightly lower effect of the gas plasma *versus* UV-C on viral air decontamination (B and C, Fig. 3 and Table 1). When the Biozone COP was tested, percentage efficiencies were significantly higher for influenza virus A (H5N2) and RSV (0.8–0.98% enhancement). The combined effects of gas plasma and internal UV, in the Biozone device brought a high level of inactivation rate. These particular features have never been described before. Future investigations will explore the efficiency of Biozone COP on contaminated surfaces.

Altogether, the results of this study revealed marked differences in inactivation rates amongst A (H5N2), hPIV-3 and RSV. The higher inactivation rates, in the three experimental conditions, were always obtained for hPIV-3. Lower inactivation rates were obtained for influenza virus A (H5N2) and RSV (Table 1). Because of the initial infectious titers and the sensitivity of the viral assays varied, it is difficult to determine if these differences represented a specific susceptibility to the disinfection processes or just reflect

Please cite this article in press as: Terrier O, et al. Cold oxygen plasma technology efficiency against different airborne respiratory viruses. *J Clin Virol* (2009), doi:10.1016/j.jcv.2009.03.017

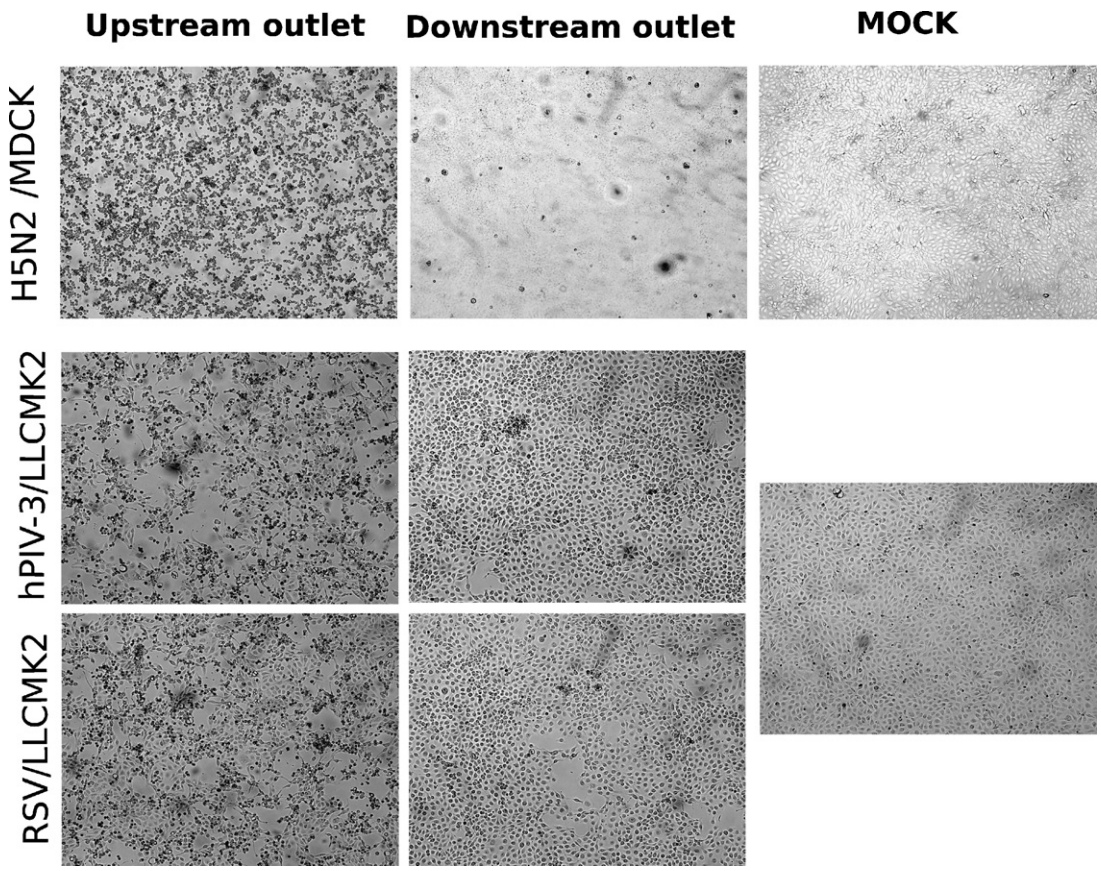

Fig. 4. Monitoring of the cytopathic effect obtained with infection of MDCK or LLC-MK2 cells with samples harvested at the upstream and downstream outlets when the internal Biozone COP was switched on.

variations or our experimental conditions. However, initial infectious titers for hPIV-3 and RSV were quite similar and the same cellular system was used. Differences of inactivation rates could be explain by viral features like the protein and lipid composition of the particle or the relative importance of the viral matrix, for example. The possible link between structural characteristics and susceptibility to UV and or plasma will be further investigated. The efficiency against non-enveloped virus, e.g. adenovirus will be also explored.

Cold oxygen plasma technology appears to be an efficient air decontamination tool to protect human population against airborne infections. The Biozone COP commercial apparatuses are already used to prevent dissemination of multiresistant bacteria in hospital, for example. In a similar way, this new-engineered method could be used to control the airborne transmission of viruses in high-risks settings, like hospital wards for example. With the recent emergence of viral respiratory pathogens such as avian influenza virus A (H5N1), the COP technology could constitute a precious tool for the reduction of influenza transmission in the various consultation settings implemented for the management of cases during a pandemic.

Conflict of interest

The authors declare that they have no conflict of interests.

Acknowledgments

The authors would like to thank all the "respiratory viruses" team in VirPAth Lab for their support. A preliminary report of this work has been presented previously at the European Society Clinical Virology meeting, at Saariselska, Finland the 12–14th March of 2008. The authors would like to acknowledge the Organising Committee and all the participants for helpful questions and discussions, which have motivated the redaction of this article. *Funding source*: CNRS and Biozone Europe fundings.

References

1. Welliver RC. Review of epidemiology and clinical risk factors for severe respiratory syncytialvirus (RSV) infection. *J Pediatr* 2003;**143**(November (5 Suppl.)):S112–7.
2. Henrickson KJ. Parainfluenza viruses. *Clin Microbiol Rev* 2003;**16**(April (2)):242–64.
3. http://www.cdc.gov/rsv/about/infection.html (10.12.2008).
4. Durbin AP, Karron RA. Progress in the development of respiratory syncytial virus and parainfluenza virus vaccines. *Clin Infect Dis* 2003;**37**(December (12)):1668–77.
5. Cox NJ, Subbarao K. Global epidemiology of influenza: past and present. *Annu Rev Med* 2000;**51**:407–21.
6. http://www.who.int/csr/disease/influenza/pandemic/en/ (10.12.2008).
7. Goldmann DA. Transmission of viral respiratory infections in the home. *Pediatr Infect Dis J* 2000;**19**(October (10 Suppl.)):S97–102.
8. Ansari SA, Springthorpe VS, Sattar SA, Rivard S, Rahman M. Potential role of hands in the spread of respiratory viral infections: studies with human parainfluenza virus 3 and rhinovirus 14. *J Clin Microbiol* 1991;**29**(October (10)):2115–9.
9. Liu R, Huza MA. Filtration and indoor air quality: a practical approach. *ASHRAE J* 1995;**37**:18.
10. Mitchell BW, King DJ. Effect of negative air ionization on airborne transmission of Newcastle disease virus. *Avian Dis* 1994;**38**(October–December(4)):725–32.
11. Brickner PW, Vincent RL, First M, Nardell E, Murray M, Kaufman W. The application of ultraviolet germicidal irradiation to control transmission of airborne disease: bioterrorism countermeasure. *Public Health Rep* 2003;**118**(March–April (2)):99–114.
12. Guillard C, Bui T-H, Felix C, Moules V, Lina B, Lejeune P. Microbiological disinfection of water and air by photocatalysis. *CR Chim* 2007;**11**(January–February (1–2)):107–13.

13. Paschoalino MP, Jardim WF. Indoor air disinfection using a polyester supported TiO photo-reactor. *Indoor Air* 2008;**18**(December (6)):473–9.
14. Heindel TH, Streib R, Botzenhart K. Effect of ozone on airborne microorganisms. *Zentralbl Hyg Umweltmed* 1993;**194**(September (5–6)): 464–80.
15. Moisan M, Barbeau J, Moreau S, Pelletier J, Tabrizian M, Yahia LH. Low-temperature sterilization using gas plasmas: a review of the experiments and an analysis of the inactivation mechanisms. *Int J Pharm* 2001;**226**(September (1–2)):1–21.
16. Nelson CL, Berger TJ. Inactivation of microorganisms by oxygen gas plasma. *Curr Microbiol* 1989;(18):275–6.
17. Terrier O, Cartet G, Ferraris O, Morfin F, Thouvenot D, Hong SS, et al. Characterization of naturally occurring parainfluenza virus type 2 (hPIV-2) variants. *J Clin Virol* 2008;**43**(September (1)):86–92.
18. Reed L, Muench H. A simple method of estimating fifty percent endpoints. *Am J Hygiene* 1938;**27**:493–7.
19. Yang S, Lee GW, Chen CM, Wu CC, Yu KP. The size and concentration of droplets generated by coughing in human subjects. *J Aerosol Med* 2007;**20**(Winter (4)):484–94.
20. Fabian P, McDevitt JJ, DeHaan WH, Fung RO, Cowling BJ, Chan KH, et al. Influenza virus in human exhaled breath: an observational study. *PLoS One* 2008;**3**(July (7)):e2691.
21. Verreault D, Moineau S, Duchaine C. Methods for sampling of airborne viruses. *Microbiol Mol Biol Rev* 2008;**72**(September (3)):413–44.
22. Jensen MM. Inactivation of airborne viruses by ultraviolet irradiation. *Appl Microbiol* 1964;**12**(September):418–20.
23. Hoff JC. *Inactivation of Microbial agents by Chemical Disinfectants. EPA 600 S2-86 067. Office of Water*. Washington, DC: US Environmental Protection Agency; 1986.
24. Murray BK, Ohmine S, Tomer DP, Jensen KJ, Johnson FB, Kirsi JJ, et al. Virion disruption by ozone-mediated reactive oxygen species. *J Virol Methods* 2008;**153**(October (1)):74–7.

Please cite this article in press as: Terrier O, et al. Cold oxygen plasma technology efficiency against different airborne respiratory viruses. *J Clin Virol* (2009), doi:10.1016/j.jcv.2009.03.017

BioZone™ Destroys H5N1 Viruses

- A reduction of 5.7 logs (99.9998%) in less than 0.44 seconds

The effectiveness of BioZone™ technology in destroying H5N1 virus

Introduction: This is a summary of the tests performed to measure the effectiveness of BioZone™ technology in destroying airborne H5N1 avian influenza virus. The complete report is available upon request.

Laboratory: The tests were performed by The Centre National de la Recherche Scientifique (CNRS, The National Scientific Research Centre under the authority of France's Ministry of Research) in bio safety level 3 laboratory in Lyon, France - one of the World Health Organization (WHO) collaborative center for Avian and human influenza viruses.

Method: Influenza strain A/Finch/England/2051/91 H5N2 (316.000.000 viruses/ml) was sprayed as an aerosol into an inlet leading into a purification chamber. The first samples were collected from the inlet before the aerosol entered the purification chamber. In the chamber the virus aerosol was subjected to UV light and photo plasma-based BioZone™ technology for 0.44 seconds, after which the second samples were collected from the outlet. The concentration was then calculated using the "Reed and Muench" statistical method.

Destroys **99.9998%** of H5N1

Results: The tests show that BioZone™ technology destroys the strain of H5N1 virus, reaching 5.7 logs (99.9998%) reduction rate in less than 0.44 seconds.

About BioZone Scientific International

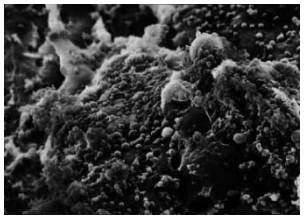

Company: With over a decade of experience in its field, BioZone Scientific International (BSI) researches, develops and manufactures technology-based solutions for microbial contaminant and VOC originated hygiene and odor problems in human environments. BSI develops best-in-class solutions for specific applications in close collaboration with its customers and distributors.

BioZone solutions, based on multi-faceted technology, are extremely efficient in eradication airborne and surface micro organisms such as viruses and bacteria, mold spores, yeasts and algae as well as volatile organic compounds (VOC). Solutions range from general use products to application specific products, for uses such as public restrooms and ice machines.

Assessment of N95 respirator decontamination and re-use for SARS-CoV-2

Robert J. Fischer[1], Dylan H. Morris[2], Neeltje van Doremalen[1], Shanda Sarchette[1], M. Jeremiah Matson[1] Trenton Bushmaker[1], Claude Kwe Yinda[1], Stephanie N. Seifert[1], Amandine Gamble[3], Brandi N. Williamson[1], Seth D. Judson[4], Emmie de Wit[1], James O. Lloyd-Smith[3], Vincent J. Munster[1]

1. National Institute of Allergy and Infectious Diseases, Hamilton, MT
2. Princeton University, Princeton, NJ
3. University of California, Los Angeles, Los Angeles, CA
4. University of Washington, Seattle, WA

The unprecedented pandemic of COVID-19 has created worldwide shortages of personal protective equipment, in particular respiratory protection such as N95 respirators[1]. SARS-CoV-2 transmission is frequently occurring in hospital settings, with numerous reported cases of nosocomial transmission highlighting the vulnerability of healthcare workers[2–4]. In general, N95 respirators are designed for single use prior to disposal. Several groups have addressed the potential for re-use of N95 respirators from a mechanical or from a decontamination perspective (for a full literature overview see Supplementary Appendix).

Here, we analyzed four different decontamination methods – UV radiation (260 – 285 nm), 70ºC heat, 70% ethanol and vaporized hydrogen peroxide (VHP) – for their ability to reduce contamination with infectious SARS-CoV-2 and their effect on N95 respirator function. For each of the decontamination methods, we compared the inactivation rate of SARS-CoV-2 on N95 filter fabric to that on stainless steel, and we used quantitative fit testing to measure the filtration performance of the N95 respirators after each decontamination run and 2 hours of wear, for three consecutive decontamination and wear sessions (see Appendix). Vaporized hydrogen peroxide and ethanol yielded extremely rapid inactivation both on N95 and on stainless steel (Figure 1A). UV inactivated SARS-CoV-2 rapidly from steel but more slowly on N95 fabric, likely due its porous nature. Heat caused more rapid inactivation on N95 than on steel; inactivation rates on N95 were comparable to UV.

Quantitative fit tests showed that the filtration performance of the N95 respirator was not markedly reduced after a single decontamination for any of the four decontamination methods (Figure 1B). Subsequent rounds of decontamination caused sharp drops in filtration performance of the ethanol-treated masks, and to a slightly lesser degree, the heat-treated masks. The VHP- and UV-treated masks retained comparable filtration performance to the control group after two rounds of decontamination, and maintained acceptable performance after three rounds.

Taken together, our findings show that VHP treatment exhibits the best combination of rapid inactivation of SARS-CoV-2 and preservation of N95 respirator integrity, under the experimental conditions used here (Figure 1C). UV radiation kills the virus more slowly and preserves comparable respirator function. 70ºC dry heat kills with similar speed and is likely to maintain acceptable fit scores for two rounds of decontamination. Ethanol decontamination is not recommended due to loss of N95 integrity, echoing earlier findings[5].

All treatments, particularly UV and dry heat, should be conducted for long enough to ensure that a sufficient reduction in virus concentration has been achieved. The degree of required reduction will depend upon the degree of initial virus contamination. Policymakers can use our estimated decay rates together with estimates of degree of real-world contamination to choose appropriate treatment durations (see Appendix).

Our results indicate that N95 respirators can be decontaminated and re-used in times of shortage for up to three times for UV and HPV, and up to two times for dry heat. However, utmost care should be given to ensure the proper functioning of the N95 respirator after each decontamination using readily available qualitative fit testing tools and to ensure that treatments are carried out for sufficient time to achieve desired risk-reduction.

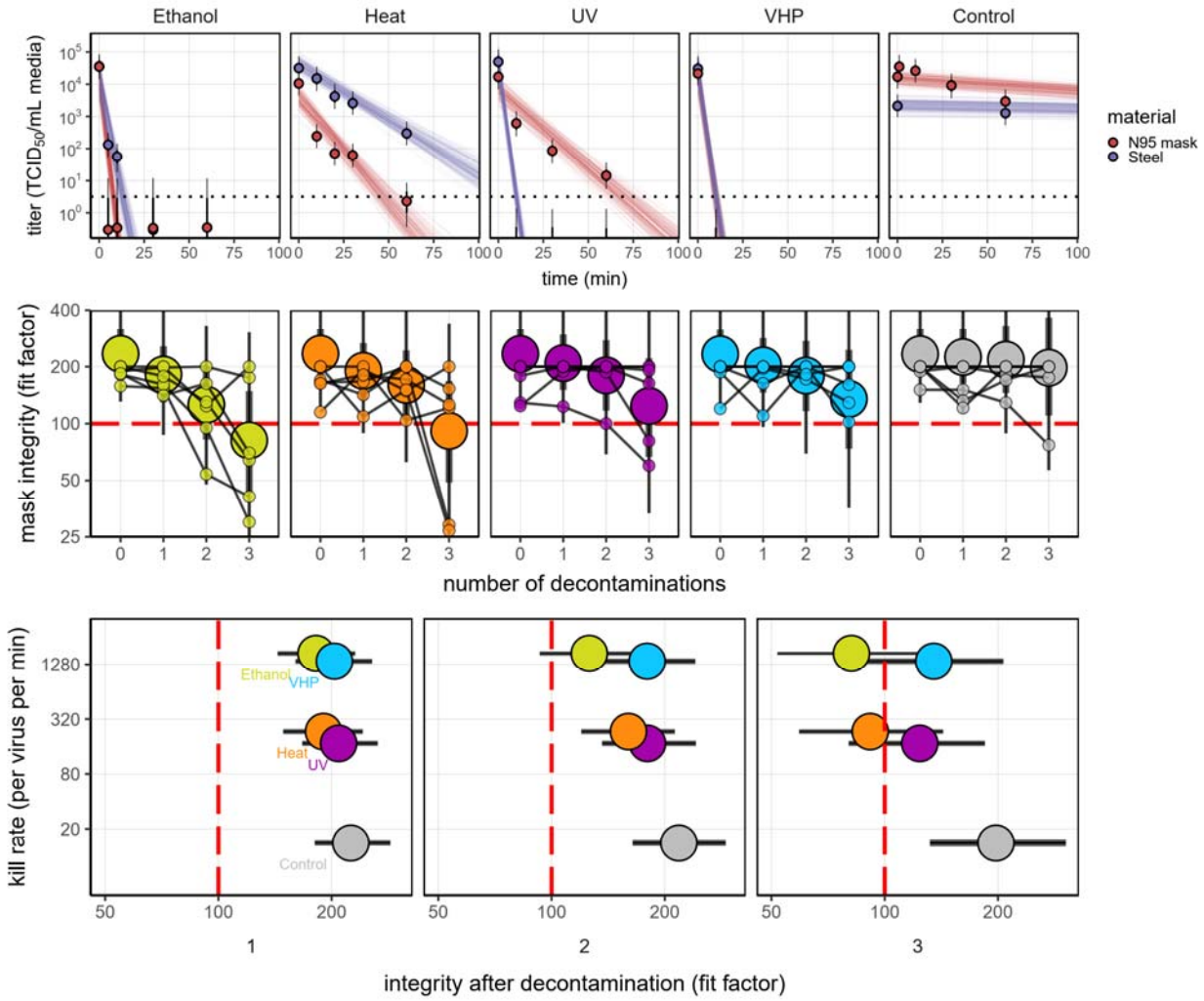

Figure 1. Decontamination of SARS-CoV-2 by four different methods. **A)** SARS-CoV-2 on N95 fabric and stainless steel surface was exposed to UV, 70 ºC dry heat, 70% ethanol and vaporized hydrogen peroxide (VHP). 50 µl of 10^5 $TCID_{50}$/mL of SARS-CoV was applied on N95 and stainless steel (SS). Samples were collected at indicted timepoints post exposure to the decontamination method for UV, heat and ethanol and after 10 minutes for VHP. Viable virus titer is shown in $TCID_{50}$/mL media on a logarithmic scale. All samples were quantified by end-point titration on Vero E6 cells. Plots show estimated mean across three replicates (dots and bars show the posterior median estimate of this mean and the posterior inter-quartile range, or IQR). Lines show predicted decay of virus titer over time (lines; 50 random draws per replicate from the joint posterior distribution of the exponential decay rate, i.e. negative

of the slope, and intercept, i.e. initial virus titer). Black dashed line shows maximum likelihood estimate titer at the Limit of Detection (LOD) of the assay: $10^{0.5}$ $TCID_{50}$/mL media. **B)** Mask integrity. Quantitative fit testing results for all the decontamination methods after decontamination and 2 hours of wear, for three consecutive runs. Data from six individual replicates (small dots) for each treatment are shown in addition to the predicted median and IQR (large dots and bars respectively) fit factor. Fit factors are a measure of filtration performance: the ratio of the concentration of particles outside the mask to the concentration inside. The measurement machine reports value up to 200. A minimal fit factor of 100 (red dashed line) is required for a mask to pass a fit test. **C)** SARS-CoV-2 decontamination performance. Kill rate (y-axis), versus mask integrity after decontamination (x-axis; bar length represents IQR). The three panels report mask integrity after one, two or three decontamination cycles.

References

1. Health C for D and R. N95 Respirators and Surgical Masks (Face Masks). FDA [Internet] 2020 [cited 2020 Apr 10]; Available from: https://www.fda.gov/medical-devices/personal-protective-equipment-infection-control/n95-respirators-and-surgical-masks-face-masks

2. McMichael TM, Currie DW, Clark S, et al. Epidemiology of Covid-19 in a Long-Term Care Facility in King County, Washington. New England Journal of Medicine 2020; in press.

3. Wu Z, McGoogan JM. Characteristics of and Important Lessons From the Coronavirus Disease 2019 (COVID-19) Outbreak in China: Summary of a Report of 72 314 Cases From the Chinese Center for Disease Control and Prevention. JAMA 2020;323(13):1239–42.

4. Livingston E, Bucher K. Coronavirus Disease 2019 (COVID-19) in Italy. JAMA [Internet] 2020 [cited 2020 Apr 10]; Available from: https://jamanetwork.com/journals/jama/fullarticle/2763401

5. Liao L, Xiao W, Yu X, Wang H, Zhao M, Wang Q. Can N95 facial masks be used after disinfection? And for how many times? [Internet]. Stanford University and 4C Air, Inc; 2020 [cited 2020 Apr 10]. Available from: https://stanfordmedicine.app.box.com/v/covid19-PPE-1-2

Table of contents:

Supplemental methods page 2
Supplemental table page 9
Supplemental references page 9
Code and data availability page 10
Acknowledgements page 10

Supplemental methods

Short literature review:

The COVID-19 pandemic has highlighted the necessity for large-scale decontamination procedures for PPE, in particular N95 respirator masks[1]. SARS-CoV-2 has frequently been detected on PPE of healthcare workers[2]. The environmental stability of SARS-CoV-2 underscores the need for rapid and effective decontamination methods[3]. Extensive literature is available for decontamination procedures for N95 respirators, using either bacterial spore inactivation tests, bacteria or respiratory viruses (e.g. influenza A virus)[4-11]. Effective inactivation methods for these pathogens and surrogates include UV, ethylene oxide, vaporized hydrogen peroxide, gamma irradiation, ozone and dry heat[4,6,8,10-13]. The filtration efficiency and N95 respirator fit has typically been less well explored, but suggest that both filtration efficiency and N95 respirator fit can be affected by the decontamination method used[12,14]. It will therefore be critical that FDA, CDC and OSHA guidelines with regards to fit testing, seal check and respirator re-use are followed[4,15-18].

Laboratory experiments

Viruses and titration

HCoV-19 nCoV-WA1-2020 (MN985325.1) was the SARS-CoV-2 strain used in our comparison[19]. Virus was quantified by end-point titration on Vero E6 cells as described previously[20]. Virus titrations were performed by end-point titration in Vero E6 cells. Cells were inoculated with 10-fold serial dilutions in four-fold of samples taken from N95 mask and stainless steel surfaces (see below). One hour after inoculation of cells, the inoculum was removed and replaced with 100 µl (virus titration) DMEM (Sigma-Aldrich) supplemented with 2% fetal bovine serum, 1 mM L-glutamine, 50 U/ml penicillin and 50 µg/ml streptomycin. Six days after inoculation, cytopathogenic effect was scored and the $TCID_{50}$ was calculated (see below). Wells presenting cytopathogenic effects due to media toxicity (e.g., due to the presence of ethanol or hydrogen peroxide) rather than viral infection were removed from the titer inference procedure.

N95 and stainless steel surface

N95 material discs were made by punching 9/16" (15 mm) fabric discs from N95 respirators, AOSafety N9504C respirators (Aearo Company Southbridge, MA). The stainless steel 304 alloy discs were purchased from Metal Remnants (https://metalremnants.com/) as described previously. 50 µL of SARS-CoV-2 was spotted onto each disc. A 0 time-point measurement was taken prior to exposing the discs to the disinfection treatment. At each sampling time-point, discs were rinsed 5 times by passing the medium over the stainless steel or through the N95 disc. The medium was transferred to a vial and frozen at -80°C until titration. All experimental conditions were performed in triplicate.

Decontamination methods

Ultraviolet light. Plates with fabric and steel discs were placed under an LED high power UV germicidal lamp (effective UV wavelength 260-285nm) without the titanium mesh plate (LEDi2, Houston, Tx) 50 cm from the UV source. At 50 cm the UVAB power was measured at 5 µW/cm^2 using a General UVAB digital light meter (General Tools and Instruments New York, NY). Plates were removed at 10, 30 and 60 minutes and 1 mL of cell culture medium added.

Heat treatment. Plates with fabric and steel discs were placed in a 70°C oven. Plates were removed at 10, 20, 30 and 60 minutes and 1 mL of cell culture medium added.

70% ethanol. Fabric and steel discs were placed into the wells of one 24 well plate per time-point and sprayed with 70% ethanol to saturation. The plate was tipped to near vertical and 5 passes of ethanol were sprayed onto the discs from approximately 10 cm. After 10 minutes,, 1 mL of cell culture medium was added.

Vaporized hydrogen peroxide (VHP). Plates with fabric and steel discs were placed into a Panasonic MCO-19AIC-PT (PHC Corp. of North America Wood Dale, IL) incubator with VHP generation capabilities and exposed to hydrogen peroxide (approximately 1000 ppm). The exposure to VHP was 10 minutes, after the inactivation of the hydrogen peroxide, the plate was removed and 1 mL of cell culture medium was added.

Control. Plates with fabric and steel discs and steel plates were maintained at 21-23°C and 40% relative humidity for up to four days. After the designated time-points, 1 mL of cell culture medium was added.

N95 mask integrity testing

N95 Mask (3M™ Aura™ Particulate Respirator 9211+/37193) integrity testing after 2 hours of wear and decontamination, for three consecutive rounds, was performed for a total of 6 times for each decontamination condition and control condition. Masks were worn by subjects and integrity was quantitatively determined using the Portacount Respirator fit tester (TSI, 8038) with the N95 companion component, following the modified ambient aerosol condensation nuclei counter quantitative fit test protocol approved by the OSHA (Occupational Safety and Health Administration, 2012). Subjects were asked to bend over for 40 seconds, talk for 50 seconds, move head from side-to-side for 50 seconds, and move head up-and-down for 50 seconds whilst aerosols on inside and outside of mask were measured. By convention, this fit test is passed when the final score is ≥100. For the N95 integrity testing, a Honeywell Mistmate humidifier (cat#HUL520B) was used for particle generation.

Statistical analyses

In the model notation that follows, the symbol ~ denotes that a random variable is distributed according to the given distribution. Normal distributions are parametrized as Normal(mean, standard deviation). Positive-constrained normal distributions ("Half-Normal") are parametrized as Half-Normal(mode, standard deviation). Normal distributions truncated to the interval [0, 1] are parameterized as TruncNormal(mode, standard deviation).

We use <Distribution Name>CDF(x | parameters) and <Distribution Name>CCDF to denote the cumulative distribution function and complementary cumulative distribution functions of a probability distribution, respectively. So for example NormalCDF(5 | 0, 1) is the value of the Normal(0, 1) cumulative distribution function at 5.

We use logit(x) and invlogit(x) to denote the logit and inverse logit functions, respectively:

$$\text{logit}(x) = \ln \frac{x}{1 - x} \qquad (1)$$

$$\text{invlogit}(x) = \frac{e^x}{1 + e^x} \qquad (2)$$

Mean titer inference

We inferred mean titers across sets of replicates using a Bayesian model. The $\log_{10}$ titers v_{ijk} (the titer for the sample from replicate k of timepoint j of experiment i) were assumed to be normally distributed about a mean μ_{ij} with a standard deviation σ. We placed a very weakly informative normal prior on $\log_{10}$ titers μ_{ij}:

$$\mu_{ij} \sim \text{Normal}(3, 3) \qquad (3)$$

We placed a weakly informative normal prior on the standard deviation:

$$\sigma \sim \text{Normal}(0, 0.5) \qquad (4)$$

We then modeled individual positive and negative wells for sample *ijk* according to a Poisson single-hit model[21]. That is, the number of virions that successfully infect cells in a given well is Poisson distributed with mean:

$$V = \ln(2)\, 10^{v} \qquad (5)$$

where v is the $\log_{10}$ virus titer in TCID_{50}, where v is the $\log_{10}$ virus titer in TCID_{50}, and the well is infected if at least one virion successfully infects a cell. The value of the mean derives from the fact that our units are TCID_{50}; the probability of infection at $v = 0$, i.e. 1 TCID_{50}, is equal to $1 - e^{-\ln(2) \times 1} = 0.5$.

Let Y_{ijkdl} be a binary variable indicating whether the l^{th} well of dilution factor d (expressed as $\log_{10}$ dilution factor) of sample *ijk* was positive (so $Y_{ijkdl} = 1$ if the well was positive and 0 otherwise), which will occur as long as at least one virion successfully infects a cell.

It follows from (5) that the conditional probability of observing $Y_{\text{ijkdl}} = 1$ given a true underlying titer $\log_{10}$ titer v_{ijk} is given by:

$$\text{L}(Y_{ijkdl} = 1 \mid v_{ijk}) = 1 - e^{-\ln(2) \times 10^{x}} \qquad (6)$$

Where

$$x = v_{ijk} - d \qquad (7)$$

is the expected concentration, measured in $\log_{10}$ $TCID_{50}$, in the dilute sample. This is simply the probability that a Poisson random variable with mean $(-\ln(2) \times 10^{x})$ is greater than 0. Similarly, the conditional probability of observing $Y_{ijkdl} = 0$ given a true underlying titer $\log_{10}$ titer v_{ijk} is given by:

$$L(Y_{ijkdl} = 0 \mid v_{ijk}) = e^{-\ln(2) \times 10^{x}} \quad (8)$$

which is the probability that the Poisson random variable is 0.

This gives us our likelihood function, assuming independence of outcomes across wells.

Virus inactivation regression

The durations of detectability depend on the decontamination treatment but also initial inoculum and sampling method, as expected. We therefore estimated the decay rates of viable virus titers using a Bayesian regression analogous to that used in van Doremalen et al., 2020[3]. This modeling approach allowed us to account for differences in initial inoculum levels across replicates as well as other sources of experimental noise. The model yields estimates of posterior distributions of viral decay rates and half-lives in the various experimental conditions – that is, estimates of the range of plausible values for these parameters given our data, with an estimate of the overall uncertainty[22].

Our data consist of 10 experimental conditions: 2 materials (N95 masks and stainless steel) by 5 treatments (no treatment, ethanol, heat, UV and VHP). Each has three replicates, and multiple time-points for each replicate. We analyze the two materials separately. For each, we denote by Y_{ijkdl} the positive or negative status (see above) for well l which has dilution d for the titer v_{ijk} from experimental condition i during replicate j at time-point k.

We model each replicate j for experimental condition i as starting with some true initial $\log_{10}$ titer $v_{ij}(0) = v_{ij0}$. We assume that viruses in experimental condition i decay exponentially at a rate λ_i over time t. It follows that:

$$v_{ij}(t) = v_{ij0} - \lambda_i t \quad (9)$$

We use the direct-from-well data likelihood function described above, except that now instead of estimating titer distribution about a shared mean μ_{ij} we estimate λ_i under the assumptions that our observed well data Y_{ijkdl} reflect the titers $v_{ij}(t)$.

Regression prior distributions

We place a weakly informative Normal prior distribution on the initial $\log_{10}$ titers v_{ij0} to rule out implausibly large or small values (e.g. in this case undetectable $\log_{10}$ titers or $\log_{10}$ titers much higher than the deposited concentration), while allowing the data to determine estimates within plausible ranges:

$$v_{ij0} \sim \text{Normal}(4.5, 2) \qquad (10)$$

We placed a weakly informative Half-Normal prior on the exponential decay rates λ_i:

$$\lambda_i \sim \text{Half-Normal}(0.5, 4) \qquad (11)$$

Our plated samples were of volume 0.1 mL, so inferred titers were incremented by 1 to convert to units of $\log_{10}$ TCID_{50}/mL.

Mask integrity estimation

To quantify the decay of mask integrity after repeated decontamination, we used a logit-linear spline Bayesian regression to estimate the rate of degradation of mask fit factors over time, accounting for the fact that fit factors are interval-censored ratios. Fit factors are defined as the ratio of exterior concentration to interior concentration of a test aerosol. They are reported to the nearest integer, up to a maximum readout of 200, but arbitrarily large true fit factors are possible as the mask performance approaches perfect filtration.

We had 6 replicate masks j for each of 5 treatments i (no decontamination, ethanol, heat, UV and VHP). Each mask j was assessed for fit factor at 4 time-points k: before decontamination, and then after 1,

243 2, and 3 decontamination cycles. We label the control treatment $i = 0$. So we denote by F_{ijk} the fit factor

244 for the j^{th} mask from the i^{th} treatment after k decontaminations (with $k = 0$ for the initial value).

245 We first converted fit factors F_{ijk} to the equivalent observed filtration rate Y_{ijk} by:

246 $$Y = 1 - 1/F \qquad (12)$$

Observation model and likelihood function

We modeled the censored observation process as follows. logit(Y_{ijk}) values are observed with Gaussian error about the true filtration logit(p_{ijk}), with an unknown standard deviation σ_o, and then converted to fit factors, which are then censored:

$$\text{logit}(Y_{ijk}) \sim \text{Normal}(\text{logit}(p_{ijk}), \sigma_o) \qquad (13)$$

Because our reported fit factors are known to be within integer values and right-censored at 200, for $F_{ijk} \geq 200$ we have a conditional probability of observing the data given the parameters of

$$\text{L}(F_{\text{ijk}} \mid p_{ijk}, \sigma_o) = \text{NormalCCDF}(\text{logit}(1 - 1/200) \mid \text{logit}(p_{ijk})\ \sigma_o) \qquad (14)$$

That is, we calculate the probability of observing a value of F greater than or equal to 200 (equivalent a value of Y greater than or equal to 1 – 1/200), given our parameters.

For $1.5 \leq F_{ijk} < 200$, we first calculate the upper and lower bounds of our observation $Y^{+}_{ijk} = 1 - 1 / (F_{\text{ijk}} - 0.5)$ and $Y^{-}_{ijk} = 1 - 1 / (F_{ijk} - 0.5)$. Then:

$$\text{L}(F_{\text{ijk}} \mid p_{ijk}, \sigma_o) = \text{NormalCDF}(\text{logit}(Y^{+}_{ijk}) \mid \text{logit}(p_{ijk})\ \sigma_o) -$$

$$\text{NormalCDF}(\text{logit}(Y^{-}_{ijk}) \mid \text{logit}(p_{ijk})\ \sigma_o) \qquad (15)$$

That is, we calculate the probability of observing a value between Y^{+}_{ijk} and Y^{-}_{ijk}, given our parameters.

Decay model

We assumed that each mask had some true initial filtration rate p_{ij0}. We assumed that these were logit-normally distributed about some unknown mean mask initial filtration rate p_{avg} with a standard deviation σ_p, that is:

$$\text{logit}(p_{ij0}) \sim \text{Normal}\ (\text{logit}(p_{avg}), \sigma_p) \qquad (16)$$

We then assumed that the logit of the filtration rate, logit(p_{ijk}), decreased after each decontamination by a quantity $d_{0k} + d_{ik}$, where d_{0k} is natural degradation during the k^{th} trial in the absence of

decontamination (i.e. the degradation rate in the control treatment, $i = 0$), and d_{ik} is the additional degrading effect of the k^{th} decontamination treatment of type $i > 0$). So for $k = 1, 2, 3$ and $i > 0$:

$$\text{logit}(p_{ijk}) = \text{logit}(p_{ij(k-1)}) - (d_{0k} + d_{ik}) + \varepsilon_{ijk} \qquad (17)$$

where ε_{ijk} is a normally-distributed error term with an inferred standard deviation σ_ε:

$$\varepsilon_{ijk} \sim \text{Normal}(0, \sigma_\varepsilon) \qquad (18)$$

And for the control $i = 0$:

$$\text{logit}(p_{0jk}) = \text{logit}(p_{0j(k-1)}) - d_{0k} + \varepsilon_{0jk} \qquad (19)$$

Model prior distributions

We placed a weakly informative Half-Normal prior on the control degradation rate d_0:

$$d_0 \sim \text{Half-Normal}(0, 0.5) \qquad (20)$$

We placed a weakly informative Half-Normal prior on the non-control degradation rates d_i, $i > 0$:

$$d_i \sim \text{Half-Normal}(0.25, 0.5) \qquad (21)$$

reflecting the conservative assumption that decontamination should degrade the mask at least somewhat.

We placed a Truncated Normal prior on the mean initial filtration p_{avg}:

$$p_{avg} \sim \text{TruncNormal}(0.995, 0.02) \qquad (22)$$

The mode of 0.995 corresponds to the maximum measurable fit factor of 200. The standard deviation of 0.02 leaves it plausible that some masks could start near or below the minimum acceptable threshold fit factor of 100, which corresponds to a p of 0.99.

We placed weakly informative Half-Normal priors on the logit-space standard deviations σ_p, σ_ε, and σ_o. σ_p reflects variation in individual masks' initial filtration about p_{avg}. σ_ε reflects variation in mask's true degree of degradation between decontaminations about the expected decay, and σ_o reflects noise in the observation process.

$$\sigma_p, \sigma_\varepsilon, \sigma_o \sim \text{Half-Normal}(0, 0.5) \quad (23)$$

We chose a standard deviation of 0.5 for the priors because a standard deviation of 1.5 (i.e. 3 σ in the prior) in logit space corresponds to probability values being uniformly distributed between 0 and 1; we therefore wish to tell our model not to use larger standard deviations, as these squash all p_{ijk} to one of two modes, one at 0 and one at 1[23].

Markov Chain Monte Carlo Methods

For all Bayesian models, we drew posterior samples using Stan (Stan Core Team 2018), which implements a No-U-Turn Sampler (a form of Markov Chain Monte Carlo), via its R interface RStan. We ran four replicate chains from random initial conditions for 2000 iterations, with the first 1000 iterations as a warmup/adaptation period. We saved the final 1000 iterations from each chain, giving us a total of 4000 posterior samples. We assessed convergence by inspecting trace plots and examining $\hat{R}$ and effective sample size (n_{eff}) statistics.

Supplemental table

Table S1. Effect of decontamination method on SARS-CoV-2 viability and N95 mask integrity.

		half-life (min)			time to one thousandth (min)			time to one millionth (min)		
Treatment	**Material**	**median**	**2.5%**	**97.5%**	**median**	**2.5%**	**97.5%**	**median**	**2.5%**	**97.5%**
Control	N95 mask	78	65.3	89.7	777	650	894	1.55e+03	1.3e+03	1.79e+03
	Steel	286	243	324	2.85e+03	2.42e+03	3.23e+03	5.7e+03	4.84e+03	6.45e+03
Ethanol	N95 mask	0.639	0.55	0.721	6.37	5.49	7.19	12.7	11	14.4
	Steel	1.06	0.888	1.23	10.6	8.85	12.2	21.2	17.7	24.5
Heat	N95 mask	4.64	3.87	5.41	46.3	38.5	53.9	92.6	77	108
	Steel	8.83	7.49	10.1	88	74.7	101	176	149	201
UV	N95 mask	6.26	5.31	7.15	62.4	52.9	71.2	125	106	142
	Steel	0.733	0.649	0.802	7.31	6.47	7.99	14.6	12.9	16
VHP	N95 mask	0.78	0.685	0.858	7.78	6.82	8.55	15.6	13.6	17.1
	Steel	0.765	0.669	0.843	7.63	6.67	8.4	15.3	13.3	16.8

Code and data availability

Code and data to reproduce the Bayesian estimation results and produce corresponding figures are archived online at OSF: and available on Github:

Acknowledgements

We would like to thank Madison Hebner, Julia Port, Kimberly Meade-White, Irene Offei Owusu, Victoria Avanzato and Lizzette Perez-Perez for excellent technical assistance. This research was supported by the Intramural Research Program of the National Institute of Allergy and Infectious Diseases (NIAID), National Institutes of Health (NIH). JOL-S and AG were supported by the Defense Advanced Research Projects Agency DARPA PREEMPT # D18AC00031 and the UCLA AIDS Institute and Charity Treks, and JOL-S was supported by the U.S. National Science Foundation (DEB-1557022), the Strategic Environmental Research and Development Program (SERDP, RC□2635) of the U.S. Department of Defense. Names of specific vendors, manufacturers, or products are included for public health and informational purposes; inclusion does not imply endorsement of the vendors, manufacturers, or products by the US Department of Health and Human Services.

Supplemental references

1. Ranney ML, Griffeth V, Jha AK. Critical Supply Shortages - The Need for Ventilators and Personal Protective Equipment during the Covid-19 Pandemic. N Engl J Med 2020.
2. Ong SWX, Tan YK, Chia PY, et al. Air, Surface Environmental, and Personal Protective Equipment Contamination by Severe Acute Respiratory Syndrome Coronavirus 2 (SARS-CoV-2) From a Symptomatic Patient. JAMA 2020.
3. van Doremalen N, Bushmaker T, Morris DH, et al. Aerosol and Surface Stability of SARS-CoV-2 as Compared with SARS-CoV-1. N Engl J Med 2020.
4. Decontamination and Reuse of Filtering Facepiece Respirators . 2020. (Accessed 4/5/2020, 2020, at https://www.cdc.gov/coronavirus/2019-ncov/hcp/ppe-strategy/decontamination-reuse-respirators.html.)
5. Final Report for the Bioquell Hydrogen Peroxide Vapor (HPV) Decontamination for Reuse of N95 Respirators. 2016. at https://www.fda.gov/media/136386/download.)
6. Fisher EM, Shaffer RE. A method to determine the available UV-C dose for the decontamination of filtering facepiece respirators. J Appl Microbiol 2011;110:287-95.
7. Heimbuch BK, Kinney K, Lumley AE, Harnish DA, Bergman M, Wander JD. Cleaning of filtering facepiece respirators contaminated with mucin and Staphylococcus aureus. Am J Infect Control 2014;42:265-70.
8. Heimbuch BK, Wallace WH, Kinney K, et al. A pandemic influenza preparedness study: use of energetic methods to decontaminate filtering facepiece respirators contaminated with H1N1 aerosols and droplets. Am J Infect Control 2011;39:e1-9.
9. Lin TH, Tang FC, Hung PC, Hua ZC, Lai CY. Relative survival of Bacillus subtilis spores loaded on filtering facepiece respirators after five decontamination methods. Indoor Air 2018.
10. Mills D, Harnish DA, Lawrence C, Sandoval-Powers M, Heimbuch BK. Ultraviolet germicidal irradiation of influenza-contaminated N95 filtering facepiece respirators. Am J Infect Control 2018;46:e49-e55.

11. Viscusi DJ, Bergman MS, Eimer BC, Shaffer RE. Evaluation of five decontamination methods for filtering facepiece respirators. Ann Occup Hyg 2009;53:815-27.
12. Avilash Cramer ET, Sherryl H Yu, Mitchell Galanek, Edward Lamere, Ju Li, Rajiv Gupta, Michael P Short. disposable N95 masks pass qualitative fit-test but have decreases filtration efficiency after cobalt-60 gamma irradiation. MedRxiv.
13. Chemical Disinfectants, Guideline for Disinfection and Sterilization in Healthcare Facilities. 2008. at https://www.cdc.gov/infectioncontrol/guidelines/disinfection/disinfection-methods/chemical.html#Hydrogen.)
14. Lin TH, Chen CC, Huang SH, Kuo CW, Lai CY, Lin WY. Filter quality of electret masks in filtering 14.6-594 nm aerosol particles: Effects of five decontamination methods. PLoS One 2017;12:e0186217.
15. N95 Respirators and Surgical Masks (Face Masks). 2020. (Accessed 4/5/2020, 2020, at https://www.fda.gov/medical-devices/personal-protective-equipment-infection-control/n95-respirators-and-surgical-masks-face-masks.)
16. Temporary Enforcement Guidance - Healthcare Respiratory Protection Annual Fit-Testing for N95 Filtering Facepieces During the COVID-19 Outbreak. 2020. at https://www.osha.gov/memos/2020-03-14/temporary-enforcement-guidance-healthcare-respiratory-protection-annual-fit.)
17. User Seal Check Procedures (Mandatory). 2020. (Accessed April 11, 2020, at https://www.osha.gov/laws-regs/regulations/standardnumber/1910/1910.134AppB1.)
18. Respirator Fit Testing [WWW Document]. U. S. Dep. Labo. 2012. at https://www.osha.gov/video/respiratory_protection/fittesting_transcript.html (accessed 4.10.20).)
19. Holshue ML, DeBolt C, Lindquist S, et al. First Case of 2019 Novel Coronavirus in the United States. N Engl J Med 2020.
20. van Doremalen N, Bushmaker T, Munster VJ. Stability of Middle East respiratory syndrome coronavirus (MERS-CoV) under different environmental conditions. Euro Surveill 2013;18.
21. Brownie C, Statt J, Bauman P, et al. Estimating viral titres in solutions with low viral loads. Biologicals 2011;39:224-30.
22. Gelman A. Bayesian data analysis. Third edition. ed. Boca Raton: CRC Press; 2014.
23. Northrup JM, Gerber BD. A comment on priors for Bayesian occupancy models. PLoS One 2018;13:e0192819.